PHYSICAL REVIEW A **72**, 010701(R) (2005)

Interference phenomena associated with electron-emission from H_2 by (1–5)-MeV H^+ impact

S. Hossain,[1] A. L. Landers,[1] N. Stolterfoht,[2] and J. A. Tanis[1]
[1]*Western Michigan University, Kalamazoo, Michigan 49008, USA*
[2]*Hahn-Meitner-Institut Berlin GmbH, D-14109 Berlin, Germany*
(Received 24 March 2005; published 1 July 2005)

Primary and secondary interference structures attributed to coherent electron emission from the identical atomic centers of H_2 have been observed in the velocity distributions of ejected electrons resulting from (1–5)-MeV H^+ impact. The primary interference structures are found to depend on the projectile velocity, in addition to the previously observed dependence on electron ejection angle. In contrast, the secondary structures, attributed to intramolecular scattering, do not change with projectile velocity and show only slight variations with the electron ejection angle. The data also provide evidence for significantly higher-frequency structures for which no explanation currently exists.

DOI: 10.1103/PhysRevA.72.010701 PACS number(s): 34.50.Fa, 32.80.Fb

The observation [1] of oscillatory structures in the velocity distributions of electrons ejected from H_2 confirmed long-standing predictions [2–4] of interferences resulting from coherent emission from identical atomic centers, and led to theoretical [5–7] formulations of this phenomenon. Subsequent studies revealed the angular dependence of the oscillatory structures [8], and the existence of secondary oscillations superimposed on the main interference structures [9]. The primary structures are analogous to Young-type interferences resulting from the passage of light through closely spaced slits, while the secondary oscillations (with ~2–3 times higher frequency) have been attributed to additional scattering within the molecule [9], an effect that has no analogy in Young's two-slit experiment. The observations to date have prompted several experimental [10–14] and theoretical [15] investigations

For collisions of charged particles with H_2, electron interference effects are manifested as oscillations in the cross section for electron emission as a function of the ejected electron velocity [1,3], and can be conveniently displayed according to the relation

$$(\sigma_{H_2})_{norm} = \frac{d^2\sigma_{H_2}}{d\Omega d\varepsilon} \Big/ \frac{d^2\sigma_{2H}}{d\Omega d\varepsilon} = \int \frac{d^3\sigma_{2H}}{d\mathbf{q}d\Omega d\varepsilon}\left[1 + \frac{\sin|\mathbf{k}-\mathbf{q}|d}{|\mathbf{k}-\mathbf{q}|d}\right]d\mathbf{q} \Big/ \int \frac{d^3\sigma_{2H}}{d\mathbf{q}d\Omega d\varepsilon}d\mathbf{q}, \quad (1)$$

where the solid angle $d\Omega$ and the energy $d\varepsilon$ refer to the outgoing electron. The cross-section σ_{H_2} denotes the molecular two-center emission and σ_{2H} describes incoherent electron emission from the two H atoms. The sinusoidal term represents the interference caused by coherent emission from the two centers, where $|\mathbf{k}-\mathbf{q}|$ is the difference between the outgoing electron momentum $\mathbf{k}$ and the momentum transfer $\mathbf{q}$, and d is the molecular internuclear distance. This normalized cross-section ratio $(\sigma_{H_2})_{norm}$ is obtained after averaging over the random orientation of the internuclear H_2 axis. To compare with experiment, the right-hand side of the Eq. (1) must be integrated over $\mathbf{q}$.

In this Rapid Communication, we report interference phenomena, manifested as oscillations in the ejected electron velocity distributions, for the ionization of H_2 by (1–5)-MeV H^+ impact. These results extend previous observations by examining the unexplored dependence of the interference structures on the collision velocity, and at the same time reveal additional features associated with the interference. In the present paper, the primary oscillatory structure is found to be velocity dependent at low collision velocities, and then become nearly constant for velocities greater than ~15 a.u. In addition to the primary interference structures, as in Ref. [9], secondary structures with higher-frequencies superimposed on the main structure are observed. However, these latter oscillatory structures, attributed to interference of the primary wave with the secondary wave produced by scattering at the other atomic center, are essentially independent of the collision velocity and, furthermore, exhibit only a small dependence on the electron observation angle. Evidence for still higher-frequency structures is also seen, although the origin of these latter structures is not yet clear.

The measurements were conducted at Western Michigan University using the tandem Van de Graaff accelerator. Well-collimated beams of 1-, 3-, and 5-MeV H^+ ions and intensities 0.1–0.5 μA were directed into the scattering chamber. The H_2 target was supplied by a gas jet of ~2-mm diam, with the flow rate set to maintain a pressure of a few times 10^{-5} Torr in the scattering chamber. A parallel-plate electron spectrometer equipped with a channel electron multiplier (CEM) was used to detect ejected electrons in the energy range ~3–300 eV at observation angles 30°, 60°, 90°, and 150° relative to the incident H^+ beam direction. Magnetic fields inside the scattering chamber were minimized by shielding with a μ-metal liner. The incident beam intensity was counted downstream in a Faraday cup. The beam-induced electron background was determined by taking spectra without the target gas.

In Fig. 1, the primary oscillatory interference features are displayed as a function of the electron velocity (in atomic units) for the observation angles 30°, 90°, and 150° with respect to the incident beam direction and for 1-, 3-, and

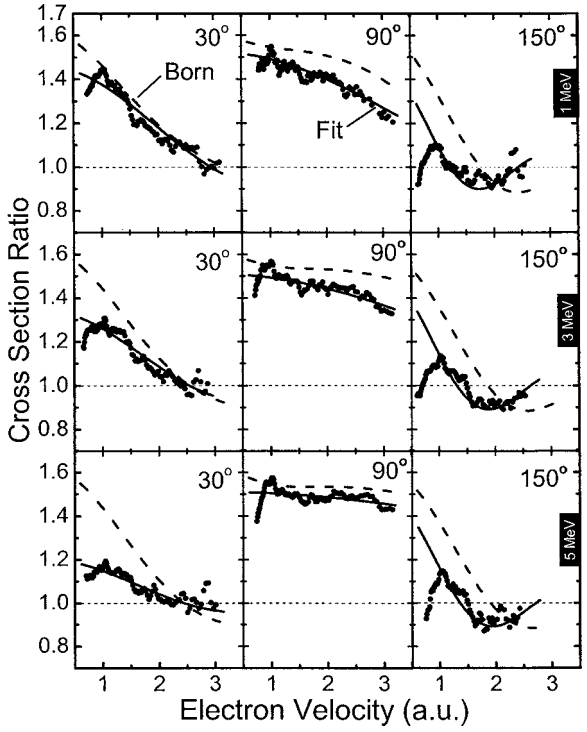

FIG. 1. Ratios of cross sections from Eq. (1) for electron emission from H_2 by 1-, 3-, and 5-MeV H^+ impact normalized to the corresponding atomic H cross sections for electron observation angles 30°, 90°, and 150°. Solid points are measured H_2 cross sections divided by theoretical Born approximation cross sections for atomic H. Dashed curves are ratios of theoretical Born cross sections for H_2 divided by those for H. The theoretical results were calculated using an analytical form for the Born cross sections obtained from hydrogenic wave functions [16,17] for atomic H. The solid curves are fits to the data using Eq. (2).

5-MeV H^+ projectiles impacting on H_2. To obtain the plotted ratios, measured doubly differential (in electron energy and observation angle) cross sections for electron emission from H_2 have been divided by corresponding theoretical Born cross sections for the ionization of atomic hydrogen [1,8] [see Eq. (1)]. Because of limited statistics, the measured cross sections are less accurate for electron velocities greater than ~2.5 a.u. (85 eV), while below ~0.5 a.u. (3.5 eV) the accuracy is limited by the difficulty of detecting very low energy electrons.

The Born approximation was used to normalize the measured electron emission from H_2 to that for two independent H atoms, and the calculated cross section ratios shown in Fig. 1 (dashed curves) were obtained by numerical integration of Eq. (1) using analytic cross sections obtained from hydrogenic wave functions [16,17] for atomic H. Because of the moderately high projectile velocities and the small Z_p (atomic number of the projectile) of the present paper, the two-center projectile-target effects [17] are expected to be small. Thus, it is fully justified to use the Born approximation to calculate the theoretical cross sections for 2H. As a check on the Born results, the calculated cross section ratios were compared with the corresponding ratios determined from continuum-distorted-wave-eikonal-initial-state (CDW-EIS)[18] calculations (not shown) and the agreement is excellent. Furthermore, cross-section ratios obtained in the impact-parameter formulation of Nagy *et al.* [5] are essentially indistinguishable from the Born results shown in Fig. 1, and from CDW-EIS results [18].

The measured interference structures in Fig. 1 show strong variations with the electron ejection angle as reported previously [8], and additionally the oscillation frequencies vary with the projectile velocity for both forward and backward angles. Similar frequency variations with projectile energy were found for 60° (results not shown). At forward angles the interference structure oscillates more slowly at 1 MeV than at 5 MeV. On the other hand, for the backward angle of 150°, the opposite dependence is seen with the interference pattern oscillating faster at the lowest projectile energy. Furthermore, the interference structure for 150° shows a significantly higher oscillation frequency than for 30° for all projectile energies. The 90° data show a collision velocity dependence similar to 150° but with a very much lower oscillation frequency, particularly for 5 MeV. At 90°, electron emission is strongly dominated by binary encounter electrons with the result that interference structures are expected to diminish [19]. The observed collision velocity dependences are in qualitative agreement with predictions of the Born approximation as given by the dashed curves, although deviations from the predicted oscillation frequencies exist. It is emphasized that cross section ratios nearly identical to the Born ratios are obtained from CDW-EIS calculations [18] and from the formulation of Nagy *et al.* [5], as already noted above. Thus, similar deviations occur between the measured ratios of Fig. 1 and these latter theories, pointing to inadequacies in each these theoretical formulations of interference phenomena.

In order to parametrize the changing frequency, an analytical function of the form

$$f(k) = A[1 + \sin(kcd)/(kcd)] + B \qquad (2)$$

was fitted to the normalized ratios of Fig. 1, a procedure that has been used in Refs. [8,9]. In this function, A and B $(A+B=1)$ are constants representing the interfering and noninterfering cross-section fractions, respectively, and c is an adjustable frequency parameter. This function is based on the impact-parameter formulation of Nagy *et al.* [5], where it is found that the argument of the sine function governing the interference term [see Eq. (1)] can be approximated by $(k \cos\theta - q_{\min})$, i.e., the electron momentum component parallel to the beam direction (θ is the electron observation angle) minus the minimum momentum $q_{\min}$ transferred in the collision. Here, $q_{\min}=\Delta E/v_p$ where ΔE is the energy transferred to the electron and v_p is the velocity of the projectile. The results of this fit, the solid curves in Fig. 1, are seen to represent very well the measured cross-section ratios.

Values of the frequency parameter c obtained from the fit function are plotted vs v_p in Fig. 2 along with the values for high-velocity ($v_p \sim 40$ a.u.) Kr^{33+} projectiles [8,9]. Also shown are the values of c determined from the Born approximation, which follow well the trends of the fit values, although for 90° and 150° the fit values are underestimated, particularly so for 150°. While the observed variations in c

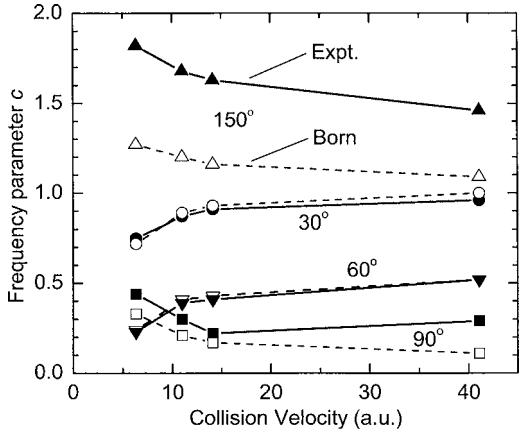

FIG. 2. Experimental and theoretical values of the primary interference frequency parameter c as a function of collision velocity v_p in atomic units (data plotted near 40 a.u. are for Kr^{33+} projectiles from Refs. [8,9]). The solid symbols are the fit values from Eq. (2) and the open symbols are results from the Born approximation (see text).

with the electron ejection angle and collision velocity can be understood in terms of the above-mentioned dependence on $(k\cos\theta - q_{\min})$, the magnitudes of c for 90° and 150° are not accurately represented by the Born theory. Moreover, since each of the theoretical formulations considered here (Born, Nagy *et al.* [5], and CDW-EIS [18]) predict nearly identical cross-section ratios, the discrepancies suggest that these theories do not properly describe the oscillatory part of the interference structure, especially for backward angles.

Closer inspection of the measured ratios shown in Fig. 1 suggests the existence of additional reproducible higher-frequency structures superimposed on the main oscillatory structure. To display these higher-frequency structures more clearly the measured cross-section ratios from Fig. 1 have been divided by their corresponding fits [from Eq. (2)] to give the results shown in Figs. 3(a) and 3(b) (cross-section ratios for 60° are not shown in Fig. 1). In these figures, the plotted ratios exhibit small amplitude (note the ordinate scale) secondary oscillations indicated by the solid curves (discussed below) as a function of the ejected electron velocity, and, additionally, suggest the existence of still weaker structures of even higher frequency. Neither the secondary nor the high-frequency structures appear to exhibit strong dependences on the collision velocity or the observation angle. It is noted that the data of Fig. 1 were taken at different times, and measurements were repeated for all collision energies and all electron observation angles. The higher-frequency structures always appeared at the same points in the spectra with nearly constant intensities. Careful attention was paid to all experimental parameters to avoid spurious instrumental effects. A detailed statistical analysis of the data was carried out to ensure that the observed structures are outside expected statistical variations [20]. Hence, there is high confidence in the accuracy of these data. Additionally, more recent measurements with improved statistics for 3-MeV $H^+ + H_2$ at 90° show similar high-frequency structures that are outside the estimated statistical uncertainties [21].

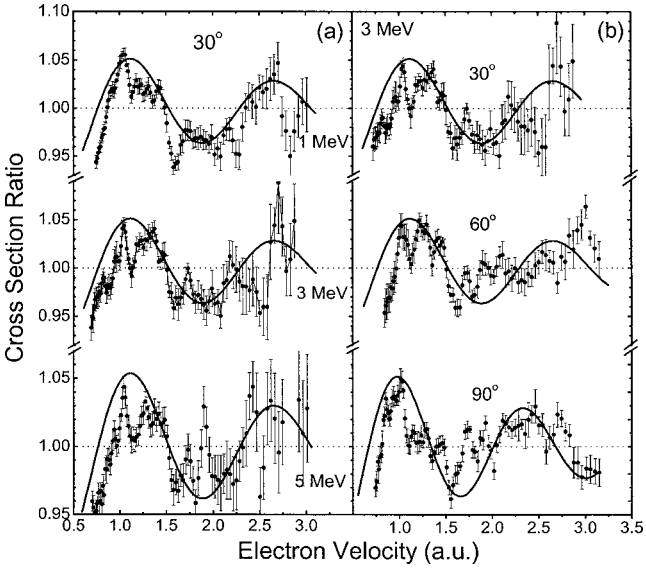

FIG. 3. Cross-section ratios of Fig. 1 divided by the corresponding fit functions [Eq. (2)] showing small amplitude secondary oscillations (solid curves) and still weaker higher-frequency structures as a function of ejected electron velocity for (a) 1-, 3-, and 5 -MeV H^+ impact at 30° observation angle and (b) observation angles of 30°, 60°, and 90° (ratios for 60° not shown in Fig. 1) for 3-MeV H^+. The solid curves were obtained by fitting a function similar to Eq. (2) to the plotted points, but with kcd replaced by $kc'd+\phi'$ (see text for details).

To quantify the secondary oscillatory structures of Figs. 3(a) and 3(b), the ratios were fit to a function similar to that of Eq. (2), but with the sine argument kcd replaced by $kc'd+\phi'$ [9], thereby allowing for a phase shift associated with these secondary structures. The results of this fitting, indicated by the solid curves in Fig. 3, give values for c' of 2.9, 2.9, 3.3, and 2.7 for the ejection angles 30°, 60°, 90°, and 150° (not shown), respectively, and a phase shift $\phi' \sim \pi$. Moreover, c' does not vary with the collision velocity as seen in Fig. 3(a). In Ref. [9] for 68 MeV/u $Kr^{33+} + H_2$ collisions similar secondary structures were found with $c' \approx 2.5$ and $\phi' \sim \pi$.

These secondary oscillations have been attributed to interference of the primary ejected electron wave with the secondary wave that results from scattering at the other atomic center [9], an effect that has no analogy in Young's two-slit experiment, and can be interpreted from phase differences using the methods of wave optics as discussed in Refs. [9,22]. The secondary interference structures are inherently different from the primary structures in that, based on the present results, there is no collision velocity dependence and at most a small dependence on the electron observation angle, based on the present results and those of Ref. [9]. Indeed, the theoretical formulations presented in Refs. [9,22] indicate the secondary oscillatory structure to be governed simply by the electron momentum k rather than by $|\mathbf{k}-\mathbf{q}|$, with the consequence that the oscillations should not depend on either the collision velocity or on the electron emission angle. This formulation predicts a secondary oscillation frequency corresponding to $c'=2$ resulting from the additional phase acquired by propagation of the primary electron wave

along the internuclear axis from one atomic center to the other. Since the determination of this expected secondary frequency in Refs. [9,22] required substantial approximation, the agreement between theory and experiment is reasonable. However, a more precise characterization of these secondary oscillations as a function of the ejected electron velocity remains a significant theoretical challenge.

Finally, we note that the ratios plotted in Fig. 3 also show evidence for structures with significantly higher frequencies. While the relatively strong peak centered near $\sim$1.0 a.u. is due to autoionization electrons from doubly excited H_2 [1,8], close inspection of Figs. 3(a) and 3(b) suggests other reproducible structures both below and above this autoionization peak. If these high-frequency structures can be confirmed by further measurements, the results would point to a heretofore unobserved aspect of electron emission from molecules.

The origin of such high-frequency structures is not obvious, however. Due to the high projectile velocity, coherent electron emission from the transient molecule formed by the passing H^+ ion and the H_2 molecule, as identified theoretically for much lower velocity 20-keV H^++H collisions [23], is unlikely. A more likely explanation for high-frequency structures is interference between direct electron emission and autoionization involving *continuum* doubly excited H_2 states $2l2\varepsilon'$ giving rise to free-free transitions [24]. Such interference was recently observed for *bound* doubly excited states in e^-+H_2 collisions [25]. The presence of the relatively large autoionization peak near 1.0 a.u. [1,8] indicates a significant probability for forming autoionizing states, an observation that is consistent with such an explanation.

In summary, we have reported the observation of electron interference effects due to coherent emission from the identical atomic centers of H_2, as manifested in the velocity distributions of electrons ejected from H_2 by (1–5)-MeV protons. The frequency of the primary oscillatory structure is found to vary with the projectile velocity for low collision velocities, reaching a nearly constant value for collision velocities above $\sim$15 a.u. Variations of the primary structure with the ejected electron observation angle are similar to those reported previously [8]. On the contrary, the frequency of the secondary interference structure, attributed to additional scattering within the molecule, does not appear to change with the projectile velocity and varies only slightly with the electron observation angle. Finally, there is the suggestion of still higher-frequency structures superimposed on the secondary oscillations, but the existence of the former structures must be further confirmed. Thus, while the primary structures are reasonably well understood, it is clear that additional experimental and theoretical work is needed to properly characterize the secondary and high frequency oscillations.

This work was supported in part by the Chemical Sciences, Geosciences, and Biosciences Division, Office of Basic Energy Sciences, U.S. Department of Energy, and by the National Science Foundation International Programs, U.S. Germany-Cooperative Research.

[1] N. Stolterfoht *et al.*, Phys. Rev. Lett. **87**, 023201 (2001).
[2] H. D. Cohen and U. Fano, Phys. Rev. **150**, 30 (1966).
[3] A. Messiah, *Quantum Mechanics* (North Holland, Amsterdam, 1970), Vol. II, p. 848.
[4] W. J. Moore, Physical Chemistry, 2nd ed. (Prentice Hall, Inc., Englewood Cliffs, NJ, 1955), pp. 236–239.
[5] L. Nagy, L. Kocbach, K. Pora, and J. P. Hansen, J. Phys. B **35**, L453 (2002).
[6] M. E. Galassi *et al.*, Phys. Rev. A **66**, 052705 (2002).
[7] L. Sarkadi, J. Phys. B **36**, 2153 (2003).
[8] N. Stolterfoht *et al.*, Phys. Rev. A **67**, 030702(R) (2003).
[9] N. Stolterfoht *et al.*, Phys. Rev. A **69**, 012701 (2004).
[10] S. Hossain *et al.*, Nucl. Instrum. Methods Phys. Res. B **205**, 484 (2003).
[11] D. Misra *et al.*, Phys. Rev. Lett. **92**, 153201 (2004).
[12] C. Dimopoulou *et al.*, Phys. Rev. Lett. **93**, 123203 (2004).
[13] O. Kamalou *et al.*, Phys. Rev. A **71**, 010702(R) (2005).
[14] B. Sulik *et al.*, Proceedings of the 23rd International Conference on Photonic Electronic and Atomic Collisions, Stockholm, Sweden, 2003, edited by J. Anton *et al.* (unpublished), p. We138.
[15] M. E. Galassi, R. D. Rivarola, and P. D. Fainstein, Phys. Rev. A **70**, 032721 (2004).
[16] D. L. Landau and E. M. Lifschitz, in *Quantum Mechanics: Non Relativistic Theory* (Pergamon Press, Reading, MA, 1958), p. 459.
[17] N. Stolterfoht, R. D. Dubois, and R. D. Rivarola, *Electron Emission in Heavy Ion-Atom Collisions* (Springer, Heidelberg, 1997).
[18] L. Gulyás, P. D. Fainstein, and A. Salin, J. Phys. B **28**, 245 (1995).
[19] N. Stolterfoht *et al.*, Phys. Rev. Lett. **80**, 4649 (1998).
[20] S. Hossain, Ph.D. dissertation, Western Michigan University, 2004 (unpublished).
[21] J. A. Tanis *et al.*, XXIVth ICPEAC, Rosario, Argentina, July 2005, Abstracts (unpublished).
[22] N. Stolterfoht and B. Sulik, in *Advances in Quantum Chemistry*, edited by J. Sabin and R. Cabrera-Trujillo (Elsevier Science, New York/Academic Press, New York, 2004), Vol. 46, pp. 307–327.
[23] J. F. Reading *et al.*, Phys. Rev. A **70**, 032718 (2004).
[24] N. Stolterfoht, Nucl. Instrum. Methods Phys. Res. B **53**, 477 (1991).
[25] J.-Y. Chesnel *et al.*, Phys. Rev. A **70**, 010701(R) (2004).